Thermophysical properties of CuNiMoMn Austempered Ductile Iron

Właściwości termofizyczne żeliwa ADI z dodatkiem Ni, Cu, Mn i Mo

Andrzej Gazda[1]

[1] *Instytut Odlewnictwa, Centrum Badań Wysokotemperaturowych, ul. Zakopiańska 73, 30-418 Kraków, Polska*
[1] *Foundry Research Institute, Center for High-Temperature Studies, ul. Zakopiańska 73, 30-418 Kraków, Poland*

E-mail: andrzej.gazda@iod.krakow.pl

Abstract

The aim of the study was to determine the thermophysical characteristics of CuNiMoMn austempered ductile iron (ADI) obtained as a result of standard, one-step heat treatment performed at various temperatures.

Temperature-dependent physical properties of structurally differentiated CuNiMoMn ADI were measured using thermal analysis techniques. Coefficient of thermal expansion, specific heat capacity, density, thermal diffusivity and thermal conductivity can be utilized in designing technological applications, developing databases and computer modeling of austempering heat treatment of ductile cast iron.

Austempering heat treatment causes a significant decrease in thermal diffusivity of ADI as compared to the initial as-cast ductile iron, in the temperature range of stability of ausferritic structure. It was found that as the temperature of isothermal transformation increases, the thermal diffusivity and thermal conductivity decreases despite an increase in the amount of carbon-enriched austenite. This can be explained by the predominant influence of fine acicular ferritic structure on the properties of heat transport in the ADI under study.

Keywords: ADI, ausferrite, thermal analysis, thermophysical properties, thermal conductivity

Streszczenie

Celem badań było wyznaczenie termofizycznych charakterystyk żeliwa sferoidalnego zawierającego pierwiastki stopowe Cu, Ni, Mo i Mn, hartowanego z przemianą izotermiczną (ADI) i wytworzonego w wyniku standardowej, jednostopniowej obróbki cieplnej w różnych temperaturach.

Zależne od temperatury właściwości fizyczne strukturalnie zróżnicowanych stopów ADI były wyznaczone za pomocą technik analizy termicznej. Współczynnik rozszerzalności cieplnej, ciepło właściwe, gęstość, przewodnictwo temperaturowe i przewodność cieplna mogą być wykorzystane w projektowaniu zastosowań technologicznych, rozwoju baz danych i w komputerowej symulacji procesów zachodzących w żeliwie sferoidalnym przy wytwarzaniu ADI.

Proces ausferrytyzacji powoduje znaczne zmniejszenie przewodnictwa temperaturowego żeliwa ADI w porównaniu do wyjściowego żeliwa sferoidalnego w stanie po odlaniu, w temperaturowym zakresie stabilności struktury ausferrytycznej. Stwierdzono, że w miarę jak rośnie temperatura przemiany izotermicznej, przewodnictwo temperaturowe i przewodność cieplna maleją, mimo że rośnie ilość austenitu wzbogaconego w węgiel. Można to wyjaśnić wpływem drobnej, iglastej struktury ferrytu na charakterystyki transportu ciepła w badanym żeliwie sferoidalnym.

Słowa kluczowe: ADI, ausferyt, analiza termiczna, właściwości termofizyczne, przewodnictwo temperaturowe

1. Introduction

Austempered ductile iron is a ductile iron subjected to heat treatment consisting of austenitizing and quenching followed by an isothermal holding – austempering. ADI has a good machinability, high strength-to-weight ratio, good wear resistance and damping capacity, and outstanding mechanical properties – toughness and fatigue strength.

The structure and mechanical properties of ADI depend on phase transformations proceeding successively during the austempering:

$$\gamma(C_o) \rightarrow \alpha_{ac} + \gamma_s(C) \tag{1}$$
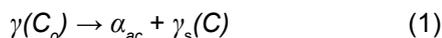
stability of ausferrite *(processing window)*

$$\gamma_s(C) \rightarrow \alpha + Fe_3C \text{ (or } \varepsilon \text{ carbide)} \tag{2}$$
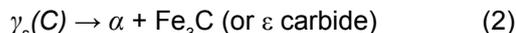
During the first stage of austenite $\gamma(C_o)$ decomposition (Eq. 1), ausferrite consisting of fine acicular ferrite α_{ac} and metastable reacted carbon-saturated austenite $\gamma_s(C)$ is created. As a result of further annealing within the processing window, optimum ausferrite with a maximum amount of fine acicular ferrite α_{ac} and reacted stable, carbon-saturated austenite $\gamma_s(C)$ is formed. The appropriate choice of austempering heat treatment parameters prevents martensite or carbides formation and results in good mechanical properties which satisfy the requirements of ASTM A 897M:1990 or BS EN 1564:1997 standards.

The prolonged time of isothermal transformation in the third stage (Eq. 2) leads to decomposition of carbon-rich austenite to ferrite and carbides.

ADI is the subject of many studies and publications, due to its attractive commercial properties and applications and its ability to analyze and further control the mechanism and kinetics of the proceeding phase transformations. There are many publications in which the authors deal with selection of optimal parameters of the standard one-step [1−13] and, with recently rising interest, complex two-step ausferritic transformation [14,15], analyzing the role of the alloying elements and ausferrite thermal stability conditions with the aim to optimize mechanical and commercial properties.

The basic parameters of heat treatment are temperature and time of austenitizing and the temperature and time of isothermal transformation. An increase in austenitizing temperature enhances the content of carbon in austenite, increasing the hardenability and increasing the time of isothermal transformation. Lowering the austenitizing temperature increases the driving force in the first stage while not affecting the processes of the precipitation of carbide in the second step, so austenitization temperature should be as low as possible and sufficient to saturate the austenite to a level of 1.1−1.3 wt. %.

Temperature of the isothermal transformation determines the microstructure and in consequence the mechanical properties of ADI. Ausferritic transformation occurring at low temperature leads to a material with a large amount of fine acicular ferrite. The structure provides high tensile strength (R_m) for low plastic properties because of the small amount of austenite saturated with carbon. Formation of martensite in the matrix is

also possible. Increase of the temperature of isothermal transformation causes deterioration of the strength and increase in elongation (A_5).

Investigations are usually limited to the analysis of the functional properties obtained for temperatures chosen from standard range of ausferritization 230−400°C and arbitrarily selected austempering times.

The objective, realized in this study was a comprehensive study of thermophysical characteristics of alloyed austempered ductile iron obtained by means of one step heat treatment.

Temperature dependent thermophysical properties of ADI, obtained under the conditions chosen based on the CCT and TTT diagrams, can be utilized in designing of technological applications or computer modeling [11,12] of austempering of ductile cast iron. It can be noticed the lack of such complex thermophysical data obtained for a wide temperature range.

Ductile cast iron, containing Cu, Ni, Mn and Mo, i.e. basic alloying elements used to improve the hardenability of ADI, was chosen for examination. Usually these elements are not all applied jointly, therefore it was accepted that the minimum contents of Mo and Mn are recommended to avoid segregation to cell boundaries where carbides can be formed, worsening the proper ausferritic structure and deteriorating mechanical properties [1].

2. Experimental

Using dynamic thermal analysis techniques such as dilatometry and DSC as well as isothermal Laser Flash Analysis (LFA), thermophysical properties of ADI with diversified structure resulting from different heat treatment parameters were determined and analysis of phase transitions accompanying the decomposition of ADI was performed. Each measurement was repeated on another test sample subjected to the same heat treatment in order to eliminate any systematic error.

Dilatometric measurements with the aim to determine a linear expansion dL/L_o, linear coefficient of thermal expansion (CTE), $\alpha = (dL/dT)/L_o$ were carried out in dilatometer Netzsch DIL 402C, with a heating rate of $q = 5$ K/min, in an atmosphere of argon 5.0 in a temperature range of RT – 1000°C.

Density ρ necessary to calculate the thermal conductivity was determined according to the formula:

$$\rho = \rho_o/(1 + dL/L_o)^3, \tag{3}$$

where ρ_o is the density at room temperature, measured by Archimedean balance.

Diversified ausferritic structure of dilatometric samples with dimensions Φ 3 mm × 10 mm was obtained using High Speed Quenching Dilatometer Linseis RITA L78.

Induction heating (cooling) of relatively small samples allows for a wide range of heating/cooling rates 0.01−150 K/s. Accurate temperature measurements were realized by using a K-type thermocouples welded to the samples. Every measurement was carried out on a new sample in the as-cast initial state.

In the initial stage of heating at low temperature, due to the temperature difference between the thermocouple and the sample, measured values are affected by systematic error and have no physical meaning; steady state is achieved at a temperature somewhat below 100°C. Above this limit the uncertainty of linear expansion and CTE amounts ±2.5−1.5% depending on temperature.

Measurements of specific heat c_p based on the reference (sapphire) method according to the c_p ASTM E 1269-05 standard were carried out using differential scanning calorimeter Netzsch 404C DSC. The samples with a weight of approx. 50 mg placed in platinum crucibles with Al_2O_3 liners were subjected to a measurement procedure consisting of heating from RT, temperature equilibration at 50°C and heating at a relatively high rate of 20 K/min in an atmosphere of argon 5.0, in the temperature range of 50−1000°C. Specific heat values calculated at low, near initial temperature, should be omitted due to unspecified errors resulting from unstable thermal conditions. The uncertainty of specific heat determination is ±2.5%.

Thermal diffusivity α study was performed using Netzsch LFA 427 laser flash equipment. The measurements were done in the temperature range of RT − 700°C in high vacuum $7 \cdot 10^{-5}$ mbar, in a step-wise manner with isothermal steps of 50°C. Test samples of standard dimensions Φ 12.7 × 2.5 mm were initially prepared by subjecting them to the ADI heat treatment in a salt bath. Each measuring point at constant temperature is the average of three measurements (laser shots), which standard deviation does not exceed 1%. Systematic uncertainty of thermal diffusivity measurements is ±3%.

Thermal conductivity was calculated according to the formula:

$$\lambda(T) = \alpha(T) \cdot c_p(T) \cdot \rho(T) \qquad (4)$$

Systematic uncertainty of thermal conductivity as a sum of partial uncertainties amounts approximately ±7−8%.

Mass fraction of the enriched with carbon austenite relative to the other remaining phases and the carbon content in austenite was determined by means of X-ray diffractometer Bruker D8 Discover.

3. Material

Material for the study was a ductile cast iron alloyed with Ni, Cu, Mo and Mn, produced in a foundry induction furnace. Composition, microstructure and method of selection of the optimal ADI heat treatment parameters of the research material whose thermophysical properties are the subject of this publication are described in detail in the previous publication [13]. Table 1 shows the chemical composition of the examined alloy.

The typical as-cast ductile iron microstructure and its description are shown in Figure 1a,b and in Table 2, respectively. Observations of microstructure were carried out using Axio Observer Z1m metallographic light microscope.

The selection of reasonable and optimal ADI one step heat treatment parameters was the analysis of CCT and TTT diagrams, which allowed greater flexibility in the design of the ADI heat treatment, supported by metallographic studies and hardness measurements, summarized in the previous paper [13]. These data, experience and data concerning the subject allowed the following values of ADI heat treatment parameters to be selected:

– Austenitization at 910°C for 40 min and cooling down to austempering temperature at the critical, i.e. minimum rate of cooling from austenitizing temperature to the temperature of isothermal transformation, which guarantees the absence of ferrite and pearlite in structure, cooling rate 5 K/s,

– Austempering at 270, 310, 350 and 390°C for 150, 120, 90 and 60 min, respectively.

Table 3 shows the mass fraction of austenite enriched with carbon and the carbon content in austenite determined by means of X-ray diffraction measurements.

Tested ADI alloys are characterized by a relatively small mass (volume) fraction of austenite and moderate saturation of carbon in austenite.

Metallographic observations of the exemplary dilatometric samples after the isothermal austenite decomposition realized at different temperatures are shown in Figure 2a−d.

Table 1. Chemical composition of the examined alloy, wt. %

Tabela 1. Skład chemiczny badanego stopu, % wag.

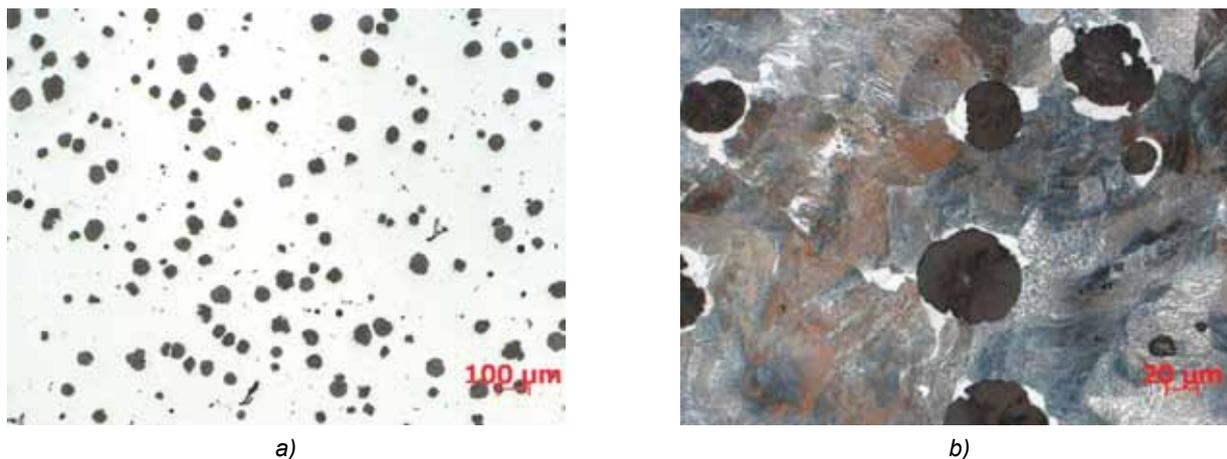| C	Si	Ni	Cu	Mn	Mo	Mg	Cr	Al	P	S
3.66	2.38	**0.85**	**0.53**	**0.21**	**0.16**	0.07	0.05	0.013	0.042	0.032

a) | *b)*

Fig. 1. Microstructure of the as-cast alloy: after polishing (a), after etching (b) [13]

Rys. 1. Mikrostruktura stopu po odlaniu: grafit, nie trawiono (a), osnowa metalowa po trawieniu (b) [13]

Table 2. Microstructure of matrix and graphite of the initial as-cast ductile cast iron [13]

Tabela 2. Mikrostruktura osnowy i grafitu wyjściowego żeliwa sferoidalnego po odlaniu [13]

| Matrix/Osnowa	Graphite PN-EN ISO 945-1:2009 / Grafit PN-EN ISO 945-1:2009	Graphite volume fraction VV, % / Udział objętościowy grafitu VV, %	Number of spheroids N, mm² / Liczba sferoidów N, mm²
Pearlite 96% / Perlit 96%	70%VI6 + 30%V6	8.1	60

Table 3. Mass fraction of the carbon-rich austenite and carbon content in the austenite

Tabela 3. Udział masowy wzbogaconego w węgiel austenitu i zawartość węgla w austenicie

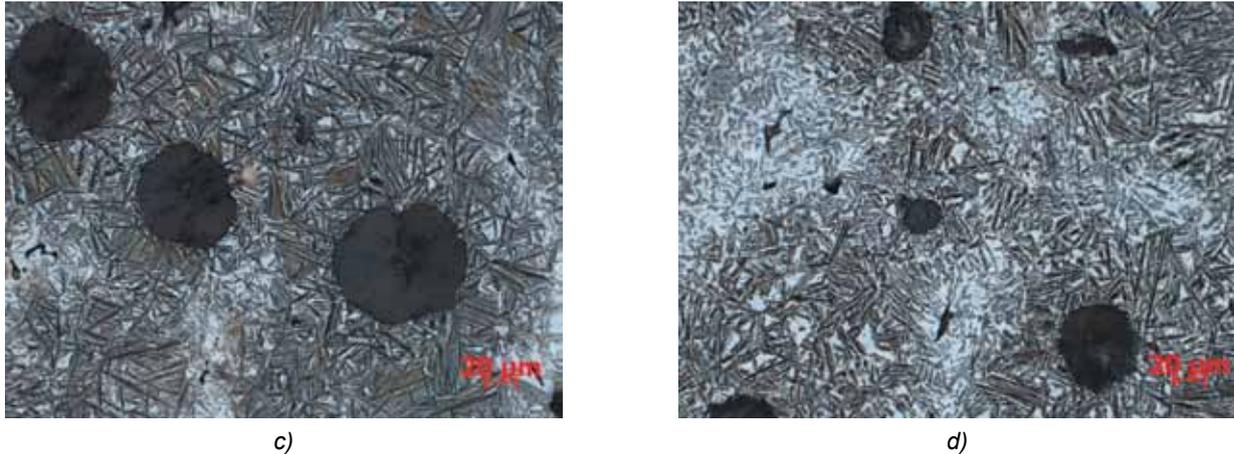| ADI	Austenite fraction, wt. % / Udział austenitu, % wag.	C_γ, wt. % / C_γ, % wag.
250°C/150 min	11.6 ±0.4	1.399 ±0.006
310°C/120 min	16.4 ±0.4	1.614 ±0.006
350°C/90 min	20.4 ±0.3	1.682 ±0.003
390°C/60 min	29.2 ±0.5	1.644 ±0.003

a) | *b)*

c) *d)*
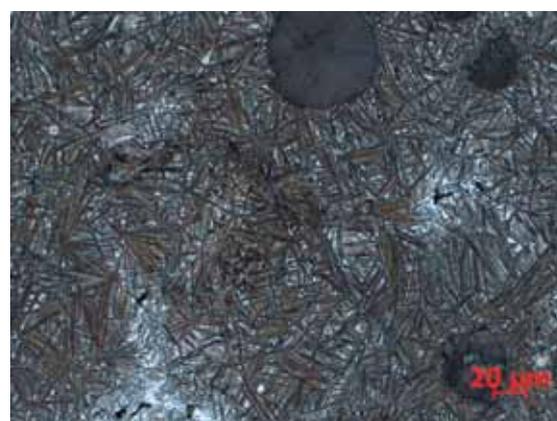
Fig. 2. Microstructure of alloys austempered at 270°C (a), 310°C (b), 350°C (c) and 390°C (d) [13]
Rys. 2. Mikrostruktura stopów po ausferrytyzacji w temperaturze 270°C (a), 310°C (b), 350°C (c) i 390°C (d) [13]

4. Thermophysical properties of ADI

Comparative DSC method of specific heat determination as well as LFA method applied for thermal diffusivity determination does not require calibration but checking measurements were performed on some standard materials – Al, Ni (c_p) and Fe, Stainless Steel 310 (α) – in order to eliminate systematic errors. Figure 3a,b presents comparisons of the measured specific heat and thermal diffusivity data with the literature data [16,17]. Assuming approx. 5% total measurements uncertainty, agreement between measuring and what is available in the literature data is appropriate.

Thermophysical properties of examined alloys were determined for the following variants of ADI heat treatment – 270°C/150 min, 310°C/120 min, 350°C/90 min and 390°C/60 min.

Figure 4a,b shows the linear expansion dL/L_o and coefficient of thermal expansion $\alpha = (dL/dT)/L_o$ of aus-

tempered ductile iron after four variants of ADI heat treatment in comparison with the relationship obtained for the as-cast alloy (bold line). Data shown in Figure 4 are necessary for calculating the thermal conductivity for the performed variants of ADI heat treatment.

The densities of austempered ductile irons, calculated using relative thermal expansion curves and room temperature densities, are shown in Figure 5a. Figure 5b shows specific heat of austempered ductile irons in comparison with the relationship obtained for the as-cast alloy (bold line).

The characteristic effects, steps and peaks in the range of 400−600°C visible in Figure 4a and Figure 4b respectively are associated with the ausferrite decomposition during heating and correspond to the 3rd stage of transformation (Eq. 2). An equivalent of these dimensional changes are the exothermal effects on the DSC curves (Fig. 5b) that reveal the complex processes associated with the decomposition of ausferrite [18].
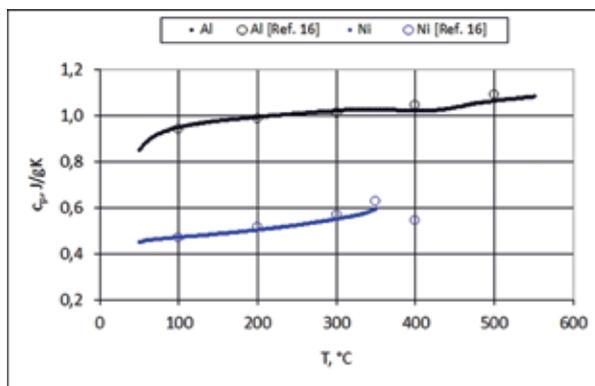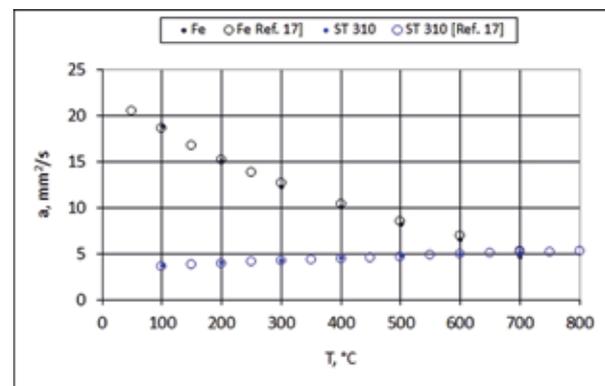
a) *b)*

Fig. 3. The comparison of measured and literature data of standard materials – specific heat (a) and thermal diffusivity (b)
Rys. 3. Porównanie zmierzonych i literaturowych danych dla wybranych materiałów – ciepło właściwe (a) i przewodność temperaturowa (b)
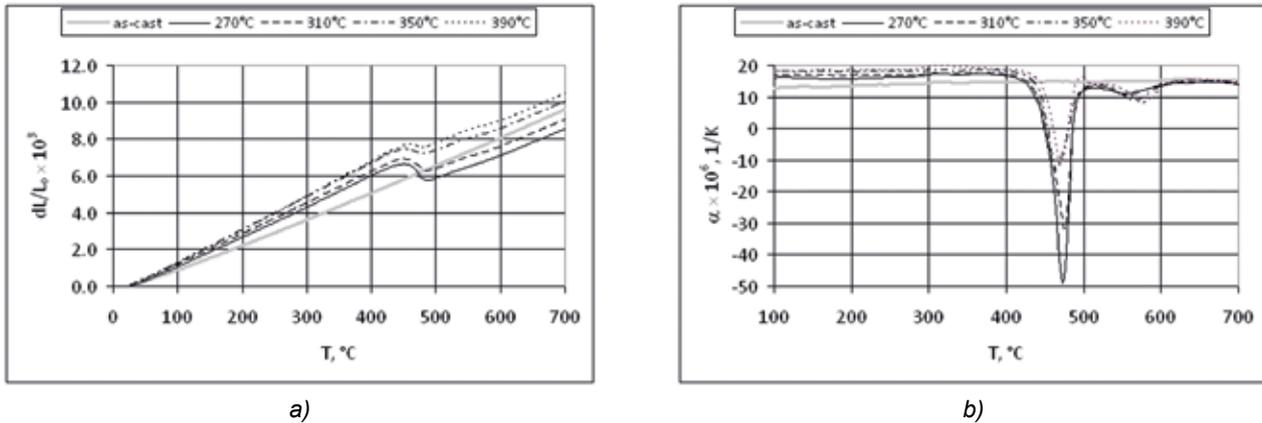
a) *b)*

Fig. 4. Thermophysical properties of austempered alloys – relative linear expansion (a), CTE (b)

Rys. 4. Właściwości termofizyczne stopów ADI – względne rozszerzenie (a), współczynnik rozszerzalności liniowej (b)
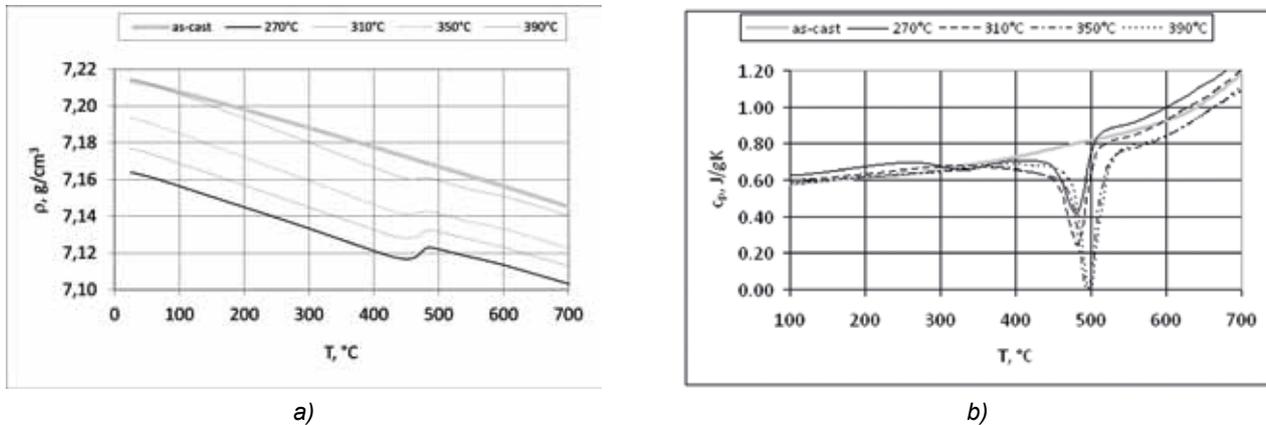

a) *b)*

Fig. 5. Thermophysical properties of austempered alloys – density (a), specific heat (b)

Rys. 5. Właściwości termofizyczne stopów ADI – gęstość (a), ciepło właściwe (b)

Lowering the austempering temperature resulting in a structure with a higher content of fine acicular ferrite and a smaller amount of carbon-enriched austenite leads to the beneficial decrease of density and the thermal expansion of the examined alloy.

Figure 6a presents temperature dependence of thermal diffusivity measured for the ADI after four variants of heat treatment – 270°C/150 min, 310°C/120 min, 350°C/90 min and 390°C/60 min.

Thermal conductivity was calculated according to the formula (3) and shown in Figure 6b in the temperature range taking into account the limitations of capability of correct determination of c_p and α at a very low temperature range. Both characteristics, thermal diffusivity and thermal conductivity are depicted in comparison with the relationship obtained for the as-cast alloy (bold line).

Generally, thermal diffusivity of ADI alloys increases with temperature and after reaching a maximum at ca 150°C decreases, similarly for graphite. Decreasing of thermal diffusivity ranging from 200°C is compliant with the results reported in [19] but thermal diffusivity values obtained in this study are lower than those presented in the cited publication. The reason is the exceptionally high percentage of carbon enriched austenite in the alloys studied in the mentioned paper.

On all the thermal diffusivity curves, in the temperature range 400−450°C, decomposition of ausferrite, according to the Eq. 2 can be observed. It is manifested by a relatively sharp increase of thermal diffusivity because of an increased amount of ferrite in the mentioned temperature range, followed by a continuous decrease at higher temperatures. Up to the temperature of the onset of decomposition, i.e. approx. 400°C, thermal diffusivity changes slightly with temperature.

It is observed that with increasing of temperature of ausferrite transformation the thermal diffusivity and thermal conductivity decrease. The lowest values of thermal diffusivity are achieved for the alloy after the treatment at the highest temperature 390°C. There is no experimentally confirmed data on this subject; the available data are informative only [19,20] without reliable literature sources, but suggest an inverse relationship, i.e. an increase of conductivity with an increase of the transformation temperature. The results obtained in this study can be explained by the fact that the expected increase of thermal diffusivity (and conductivity) resulting from
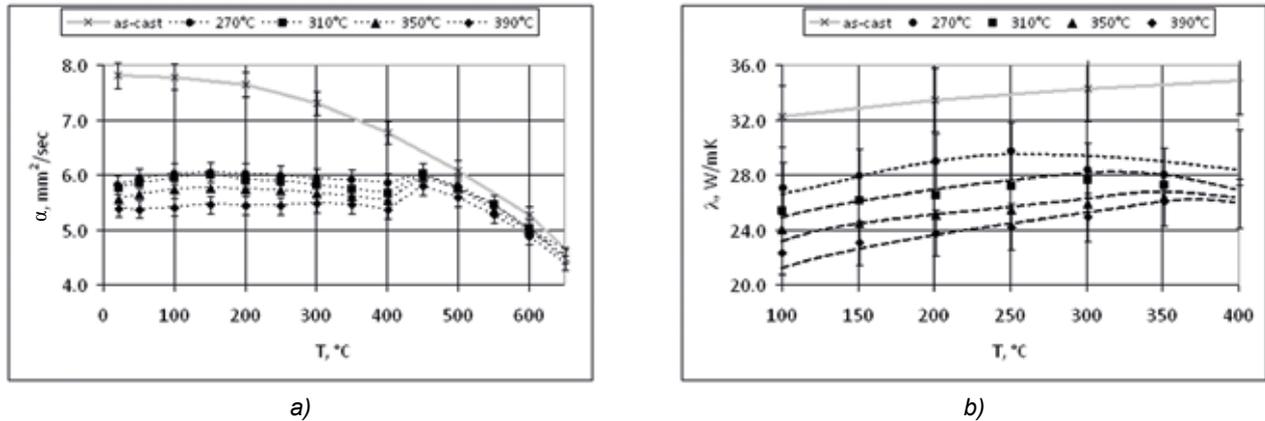
a)   *b)*

Fig. 6. Heat transport characteristics of alloys austempered at 270°C/150 min, 310°C/120 min, 350°C/90 min and 390°C/60 min – thermal diffusivity α (a), thermal conductivity λ (b)

Rys. 6. Charakterystyki transportu cieplnego stopów ADI po obróbce w temperaturze 270°C/150 min, 310°C/120 min, 350°C/90 min i 390°C/60 min – przewodność temperaturowa α (a), przewodność cieplna λ (b)

the greater volume fraction of the austenite, more saturated with the carbon has less effect than contribution of acicular ferrite generated at lower temperature in a larger amount. In fact, a relatively small volume fraction of austenite and its moderate saturation of carbon in the tested alloy may also have some significance.

This tendency is maintained in the relationship of thermal conductivity on temperature within the narrowed measuring range RT – 400°C. Above this range, the conductivity values, calculated according to the Eq. 3 are distorted by stepwise and overlapping values, sensitive to the proceeding phase transformation changes of $\alpha(T)$, $\rho(T)$ and $c_p(T)$ and have no physical meaning.

ADI treatment significantly decreases thermal diffusivity of the alloys relative to the as-cast nodular cast iron in the temperature of thermal stability of ausferrite, above this temperature values are comparable. Heat transport phenomena, induced by electrons and/or phonons mode depend on microstructure finer in ADI and acting in the same direction internal stresses, lattice defects and impurities predominant in ADI. The higher thermal diffusivity and thermal conductivity obtained at lower austempering temperature may be advantageous for machining of ADI characterized by high hardness due to better heat dissipation.

5. Conclusions

Temperature range RT – 400°C is an interval of stability of the ausferritic structure of the examined ADI alloy.

The comprehensive, dependent on temperature thermophysical properties of ADI – coefficient of thermal expansion $\alpha(T)$, specific heat $c_p(T)$, density $\rho(T)$, thermal diffusivity $a(T)$ and thermal conductivity $\lambda(T)$ were determined. Obtained data can be a contribution and

enrichment of existing thermophysical databases. They can be used for the selection of a material for particular applications when thermophysical properties are considered as a criterion of choice. These verified data can also be utilized in computer modeling of austempering heat treatment of ductile cast iron. The used approaches can be validated based on the experimental data obtained in this study for the defined alloy.

Lowering of austempering temperature leads to the beneficial decrease of density and thermal expansion of the examined alloy.

Austempering heat treatment causes a significant decrease in thermal diffusivity of ADI compared to the initial as-cast ductile iron in the temperature range of stability of the ausferritic structure.

The decrease of temperature of isothermal ausferrite transformation causes an increase of thermal diffusivity and thermal conductivity which can be explained by the predominant influence of acicular ferrite on thermal diffusivity. The higher thermal diffusivity and thermal conductivity of ADI obtained under these low temperature conditions may be beneficial compared to those obtained at higher temperatures due to better heat dissipation reducing the risk of ausferrite decomposition at elevated temperature and when machining this high hardness ADI.

The obtained results of thermal diffusivity and thermal conductivity allow for the optimization of ADI thermophysical properties to some heat transfer characteristics.

References

1. Kovacs B.V. 1994. „On the terminology and structure of ADI". *AFS Transactions* 83 : 417−420.

2. Bayati H., R. Elliott. 1999. „The concept of an austempered heat treatment processing window". *International Journal of Cast Metals Research* 11 (5) : 413−417.

3. Hafiz M. 2003. „Influence of heat treatment parameters in variable austempering temperature process on mechanical properties and fracture of SG-iron". *AFS Transactions* 111 : 03−035.

4. Erdogan M., V. Kilicli, B. Demir. 2009. „Transformation characteristics of ductile iron austempered from intercritical austenitizing temperature ranges". *Journal of Materials Science* 44 (5) : 1394−1403.

5. Amran Y., A. Katsman, P. Schaaf, M. Bamberger. 2010. „Influence of copper addition and temperature on the kinetics of austempering in ductile iron". *Metallurgical and Materials Transactions B* 41B (5) : 1052−1058.

6. Nofal A.A. 2013. „Advances in Metallurgy and Applications of ADI". *Journal of Metallurgical Engineering* 2 (1) : 1−18.

7. Pérez M.J., M.M. Cisneros, E. Valdés, H. Mancha, H.A. Calderón, R.E. Campos. 2002. „Experimental study of the thermal stability of austempered ductile irons". *Journal of Materials Engineering and Performance* 11 (5) : 519−526.

8. Batra U., S. Ray, S.R. Prabhakar. 2003. „Effect of austenitization on austempering of copper alloyed ductile iron". *Journal of Materials Engineering and Performance* 12 (5) : 597−601.

9. Yazdani S. 2006. „The influence of austempering heat treatment variables on dimensional changes of a Ni-Cu ductile iron". *Materials Science Forum* 514−516 : 702−706.

10. Vaško A. 2011. „Influence of transformation temperature on structure and mechanical properties of austempered ductile iron". *Acta Metallurgica Slovaca* 17 (1) : 45−50.

11. Kapturkiewicz W. 2004. „Modelowanie kinetyki austenityzacji żeliwa sferoidalnego perlitycznego". *Archives of Foundry* 4 (14) : 203−208.

12. Boccardo A.D., P.M. Dardati, D.J. Celentano, L.A. Godoy, M. Górny, E. Tyrała. 2016. „Numerical simulation of austempering heat treatment of a ductile cast iron". *Metallurgical and Materials Transactions B* 47B (1) : 566−575.

13. Gazda A. 2016. „Określenie optymalnych parametrów obróbki hartowania z przemianą izotermiczną żeliwa sferoidalnego Ni-Cu (Mo,Mn) na podstawie wykresów CTPc i CTPi / Determination of the optimal austempering parameters of Ni-Cu (Mo,Mn) ductile iron based on CCT and TTT diagrams". *Prace Instytutu Odlewnictwa / Transactions of the Foundry Research Institute* 56 (2) : 133−145.

14. Putatunda S.K., G.A. Bingi. 2012. „Influence of step-down austempering process on the fracture toughness of austempered ductile iron". *Journal of Materials Science and Engineering with Advanced Technology* 5 (1) : 39−70.

15. Hernández-Rivera J.L., C.G. Garay-Reyes, R.E. Campos-Cambranis, J.J. Cruz-Rivera. 2013. „Design and optimization of stepped austempered ductile iron using characterization techniques". *Materials Characterization* 83 (September 2013) : 89−96.

16. Ražnjević K. 1966. *Tablice cieplne z wykresami: dane liczbowe w układzie technicznym i międzynarodowym*. Warszawa: Wydawnictwa Naukowo-Techniczne.

17. *Netzsch Diffusivity Standards, Ver. 4.8.5*, 2008.

18. Gazda A. 2010. „Analysis of decomposition processes of ausferrite in copper-nickel austempered ductile iron". *Journal of Thermal Analysis and Calorimetry* 102 (3) : 923−930.

19. Bayati H., R. Elliott. 1999. „Influence of matrix structure on physical properties of an alloyed ductile cast iron". *Materials Science and Technology* 15 (3) : 265−277.

20. http://www.appliedprocess.com/Document/Details/TypicalPropertiesofADIMetricVersionOct2008.